Nitrogen dioxide measurement by cavity attenuated phase shift spectroscopy (CAPS) and implications in ozone production efficiency and nitrate formation in Beijing, China

Baozhu Ge,[1,2] Yele Sun,[1] Ying Liu,[3] Huabin Dong,[1] Dongsheng Ji,[1] Qi Jiang,[1,4] Jie Li,[1] and Zifa Wang[1]

Received 25 April 2013; revised 16 July 2013; accepted 10 August 2013.

[1] Nitrogen dioxide (NO_2) is a key species in studying photochemical smog and formation mechanisms of nitrate in fine particles. However, the conventional commercially available chemiluminescence (CL)-based method often has uncertainties in measuring NO_2 because of interferences with other reactive nitrogen species. In this study, an Aerodyne Cavity Attenuated Phase Shift Spectroscopy (CAPS) NO_2 monitor that essentially has no interferences with nitrogen containing species was deployed in Beijing for the first time during August 2012. The CAPS NO_2 monitor is highly sensitive with a detection limit (3σ) of 46.6 ppt for 1 min integration. The NO_2 measured by CAPS shows overall agreement with that from CL, yet large differences up to 20% were also observed in the afternoon. Further, the discrepancies of NO_2 measurements between CAPS and CL appear to be NO_z dependent with larger differences at higher NO_z concentrations (e.g., $>$ 14 ppb). As a result, the ozone production efficiency of NO_x (OPE_x) derived from the correlations of O_x-NO_z with the CL NO_2 can be overestimated by 19–37% in Beijing. The daily OPE_x calculated with the CAPS NO_2 ranges from 1.0 to 6.8 ppb/ppb with an average ($\pm1\sigma$) of 2.6 ($\pm$1.3) for the entire study. The relatively low OPE_x and the relationship between OPE_x and NO_x suggest that ozone production chemistry is VOC sensitive during summer in Beijing. Two case studies further show that high concentrations of NO_x can significantly enhance the formation of nitrate in fine particles in the presence of high O_3 and favorable meteorological conditions.

Citation: Ge, B., Y. Sun, Y. Liu, H. Dong, D. Ji, Q. Jiang, J. Li, and Z. Wang (2013), Nitrogen dioxide measurement by cavity attenuated phase shift spectroscopy (CAPS) and implications in ozone production efficiency and nitrate formation in Beijing, China, *J. Geophys. Res. Atmos.*, *118*, doi:10.1002/jgrd.50757.

1. Introduction

[2] Air pollution is a great concern in China in recent years. The roles of megacities in regional air pollution, such as photochemical smog and haze, have been extensively investigated in previous works [*Guttikunda et al.*, 2003, 2005; *Kanakidou et al.*, 2011; *Lawrence et al.*, 2007; *Madronich*, 2006; *Molina et al.*, 2010; *Molina and Molina*, 2004; *Ran et al.*, 2012]. Beijing, one of the largest cities in China and one of the top 25 world megacities, has a resident population of more than 20 million in 2012 (http://www.bjstats.gov.cn/nj/main/2012-tjnj/index.htm). The dense population and rapid economic growth have resulted in a substantial increase of anthropogenic pollutants in Beijing and regions in its vicinity, which contributes significantly to the air pollution in Beijing [*Hao et al.*, 2005; *Shao et al.*, 2006; *Wang et al.*, 2006]. It was estimated that ~74% of the ground level NO_x in Beijing is due to vehicular emissions, whereas power plants and industrial sources contribute only 2% and 13%, respectively [*Hao et al.*, 2005]. Although photochemical smog is a major air pollution issue in Beijing, the mechanisms of the formation of surface O_3 are not well known for this area; specifically with respect to the formation mechanisms of O_3 in urban versus rural areas of Beijing. *Wang et al.* [2006] found that O_3 formation in a mountainous area in the north of Beijing was limited by NO_x; however, a VOC-controlled ozone formation mechanism was dominant at the urban sites in Beijing [*Wang et al.*, 2010b]. Similarly, *Chou et al.* [2009] found that reduction of NO_x emission appeared not to be effective toward reducing O_3 concentration at an urban site in Beijing.

[1]State Key Laboratory of Atmospheric Boundary Layer Physics and Atmospheric Chemistry, Chinese Academy of Sciences, Institute of Atmospheric Physics, Beijing, China.
[2]Research Center for Environmental Changes, Academia Sinica, Taipei, Taiwan, ROC.
[3]Laboratory for Climate Studies National Climate Center, China Meteorological Administration, Beijing, China.
[4]Key Laboratory for Aerosol-Cloud-Precipitation of China Meteorological Administration, Nanjing University of Information Science and Technology, Nanjing, China.

Corresponding author: Y. Sun, State Key Laboratory of Atmospheric Boundary Layer Physics and Atmospheric Chemistry, Institute of Atmospheric Physics, Chinese Academy of Sciences, Beijing 100029, China. (sunyele@mail.iap.ac.cn)

2169-897X/13/10.1002/jgrd.50757

[3] Previous studies [*Chameides et al*., 1992; *Kleinman et al*., 1994, 2000; *Sillman*, 1999] have shown that the surface O_3 is primarily formed from photochemical reactions of VOCs and NO_x. NO_x not only plays the role of catalyst in the chain reactions for O_3 production but also is a major terminator of free radicals, which has the potential to limit the formation of O_3 in the atmosphere [*Sillman*, 1999; *Roberts et al*., 1995; *Seinfeld and Pandis*, 2006]. Since the oxidants of NO_x can be removed from the O_3-production-reaction system, *Liu et al*. [1987] defined the number of molecules of O_3 formed per NO_x as O_3 production efficiency of NO_x (OPE_x), which has been used as an important indicator in studying O_3 chemistry. *Trainer et al*. [1993] and *Kleinman et al*. [1994] found better correlations between O_3 and the oxidation products of NO_x, i.e., NO_z (= $NO_y - NO_x$) than the sum of reactive nitrogen species, NO_y, in the photochemically aged air, based on which the OPE_x was revised as $\Delta[O_3 + NO_2]/\Delta[NO_z]$. Therefore, accurate measurements of NO_y and NO_x are of importance to understand the formation mechanism of O_3 production, and hence to make the corresponding control strategies for mitigation of photochemical smog. Because of interferences of reactive nitrogen species, the OPE_x derived from the commercially standard chemiluminescence-based (called CL hereafter) instruments often has large uncertainties and represents an upper limit, especially in the photochemically aged air [*Ge et al*., 2010]. For example, *Dunlea et al*. [2007] reported an overestimation of 22% of NO_2 measured by the CL monitors compared with the collocated spectroscopic measurements in Mexico City. Such uncertainties are expected to be enlarged in the downwind areas of megacities where the production of NO_z, such as PAN and HNO_3, in the total reactive nitrogen species is more significant in comparison to urban cities.

[4] To improve the accuracy of NO_2 measurements, a NO_2 monitor utilizing Cavity Attenuated Phase Shift Spectroscopy (CAPS) was recently developed [*Kebabian et al*., 2005, 2008]. The CAPS NO_2 monitor directly measures the absorption of NO_2 at the wavelength of 450 nm and requires no conversion of NO_2 to other species. Compared to the standard commercially available CL-based NO_x analyzer, the CAPS NO_2 monitor shows much enhanced performance in terms of sensitivity, accuracy, and baseline stability [*Kebabian et al*., 2005]. In particular, the CAPS NO_2 has essentially no interferences from other nitro containing species, although small spectral interferences from 1,2-dicarbonyl compounds, such as glyoxal and methylglyoxal, are possible due to the ±20 nm band-pass centered at 440 nm [*Kebabian, et al*., 2008]. Commercially available CL analyzers are the standard type of instrument employed at surface monitoring network stations for ambient measurements of atmospheric NO_2. Ambient NO_2 analyzers employing the same CL detection scheme, yet utilizing UV photolysis with high power LEDs to convert NO_2 to NO prior to CL detection, are also commonly utilized in field research. Similar to the Aerodyne CAPS instrument, photolysis-chemiluminescence (P-CL) instruments have higher sensitivity and chemical selectivity for NO_2 than the standard commercially available NO_2 CL analyzer [*Ryerson et al.*, 2000; *Pollack et al.*, 2010; *Sadanaga et al.*, 2010]. These P-CL systems are the current recommended standard for ambient measurements of NO_2 by the Global Atmospheric Watch (GAW). Considering the above mentioned advantages of the commercially available Aerodyne CAPS NO_2 monitor compared to the standard commercial CL analyzer, evaluation of the Aerodyne CAPS NO_2 instrument as a potential resource for future NO_2 measurements has significant implications for future surface monitoring networks, especially for monitoring sites with low concentrations of NO_2 and/or where photochemical production of NO_z is intense.

[5] In this work, an Aerodyne CAPS NO_2 monitor was first deployed at an urban site in Beijing, China for in situ measurement of ambient gaseous NO_2. Here we report the results from 1 month measurement campaign during August 2012. We first evaluate the performance of the CAPS NO_2 monitor by comparing with a standard, commercial CL-based NO_x analyzer (Thermo Scientific, Model 42i). Then, we explore the impact of NO_2 measurement on the derivation of OPE_x. Further, the implications of OPE_x in O_3-NO_x-VOCs chemistry and the strategies for ozone pollution control in Beijing are discussed. Finally, two high-O_3 episodes are used to elucidate the roles of O_3 and NO_2 in the formation of secondary particulate nitrate.

2. Experimental

2.1. Sampling Site and Meteorology

[6] The ambient gaseous NO_2 was measured in situ by an Aerodyne CAPS NO_2 monitor [*Kebabian et al*., 2005, 2008] from 1 to 29 August 2012 at the Institute of Atmospheric Physics (IAP), Chinese Academy of Sciences (39°58′ 28″N, 116°22′16″E), which is located between the north 3rd and 4th Ring Road in Beijing. We have two sampling sites in this study, named site A and site B, which are approximately 50 m apart. The CAPS NO_2 monitor was deployed on the roof of a two story building (~8 m above the ground) at site A. Collocated gaseous species including NO, NO_y, and O_3 were simultaneously measured by a NO/NO_y analyzer (Thermo Scientific, 42CY) and an Ozone Analyzer (Thermo Scientific, 49C), respectively. In addition, NO, NO_2, and NO_x were measured by a CL NO/NO_2/NO_x analyzer (Thermo Electron Corporation, 42CTL) at site B. The detailed descriptions of the sampling sites are given in *Sun et al*. [2012]. The meteorological variables including temperature (T), relative humidity (RH), precipitation, solar radiation (SR), wind speed (WS) and wind direction (WD) were obtained from the meteorology tower of IAP, which is approximately 30 m away from site A and ~20 m from site B.

2.2. Cavity Attenuated Phase Shift Spectroscopy NO_2 Monitor

[7] The CAPS NO_2 monitor determines NO_2 by directly measuring optical absorption of NO_2 at 450 nm in the blue region of electromagnetic spectrum [*Kebabian et al*., 2005, 2008]. Unlike standard CL monitors, the CAPS measures the average time that the light spends within the sample cell and requires no conversion of NO_2 to other species, and thus is not sensitive to other nitro containing species (such as HNO_3, nitrate, PAN, etc.). The CAPS NO_2 system contains three major parts including a blue light emitting diode (LED) as the light source, a sample cell with two high reflectivity mirrors centered at 450 nm, and a vacuum photodiode detector. The detailed principles of the CAPS system have been described elsewhere [*Kebabian et al*., 2005, 2008]. In brief, a square wave modulated LED light is input into

the first reflected mirror, after passing through the absorption cell, the light appears to be a distorted waveform which is characterized by a phase shift in comparison to the initial modulation. By measuring the amount of the phase shift (ϑ), the concentration of NO_2 (χ) can be determined using the following formula:

$$\cot\vartheta = \cot\vartheta_0 + \frac{c}{2\pi f}\alpha_{NO_2}(T,P)\chi \quad (1)$$

where c is the speed of light, f is the LED modulation frequency, T and P are the sample temperature and pressure respectively, a_{NO2} is the absorption coefficient of nitrogen dioxide at the measured T and P, and ϑ_0 is the sensor response of NO_2-free air. Although the measurement of NO_2 theoretically requires no calibration, the CAPS NO_2 monitor was calibrated using a gas mixture with the known concentration of NO_2 before the deployment because of the nonmonochromatic light source.

2.3. Instrument Operations

[8] Ambient air was drawn into the instrument via 9.525 mm Teflon tubing at a flow rate of 0.85 L/min and passed through a disposable filter cartridge to remove particulates and prevent mirror contamination prior to being introduced to the detector. In order to measure NO_2 baseline, a zero air generator that consists of a particle filter followed by a silica gel dryer, two cartridges filled by charcoal, and the mixture of charcoal and hydroquinone, respectively was used to generate NO_2-free air. During this study, the NO_2 was measured at a time resolution of 1 s. Every hour, the ambient air flow was automatically switched to NO_2-free air to conduct baseline measurements. The cell/mirror was first flushed for 45 s and then the baseline was measured for the next 90 s. Figure 1 shows the time series of NO_2 baseline measured for the entire study. Overall, the baseline was rather stable throughout the study with more than 80% of data points falling within ±0.2 ppb and is well represented by a Gaussian distribution. The detection limit, defined as three times of one standard deviation (3σ), is 0.361 ppb for 1 s time resolution, which is equivalent to 46.6 ppt for 1 min integration. The linear response range of CAPS NO_2 instrument is 15 ppt–1 ppm. In comparison to the commercial CL-based NO_x analyzer, e.g., $NO/NO_2/NO_x$ Analyzer (Model 42i, TE) and NO_x Analyzer (Model 42i-D, TE), the sensitivity of the CAPS NO_2 exceeds the CL analyzer by nearly an order of magnitude.

[9] The CL-based gas monitors were calibrated during this study. Daily zero/span checks were automatically done using dynamic gas calibrators (Model 146C) combined with zero air suppliers (Model 111) and standard gas mixtures for NO. The multipoint calibrations of NO_x 42CTL, and NO_y 42CY analyzers were made on 20 August using the standard gases, which were compared with National Institute of Standards and Technology (NIST) traceable standards (Scott Specialty Gases, USA). An O_3 calibrator (49CPS) was used to calibrate the O_3 analyzers at the site A. The calibrator is traceable to the Standard Reference Photometer maintained by World Meteorological Organization (WMO) World Calibration Centre in Switzerland. All the gaseous species above were recorded at a time resolution of 1 min, yet 5 min averaged data were presented in this study.

[10] In addition to the gaseous species measurements, an Aerodyne Aerosol Chemical Speciation Monitor (ACSM) was used to measure the mass concentration and chemical composition of nonrefractory submicron aerosol species including organics, sulfate, nitrate, ammonium, and chloride at a time resolution of ~15 min at the site A. The detailed descriptions of ACSM measurements can be found in *Sun et al*. [2012, 2013]. In addition, all the data in this study are reported at Beijing local time which equals Coordinated Universal Time (UTC) plus 8 h.

3. Result and Discussion

3.1. Intercomparison

[11] A time series of NO and NO_2 measured by the CAPS and CL instruments is presented in Figure 2. The NO measured by 42CY at site A and 42CTL at site B track each other well ($r^2 = 0.94$, Figure 3a). However, the regression slope of 0.91 suggests that the NO measured at site A appears to be systematically lower than that observed at site B, which is likely due to the calibration errors. Also, note that the differences at the two sites are larger at low ambient levels (< 1 ppb). For example, while the minimum of NO at site A is approximately 0.4 ppb, which is close to the detection limit of 0.4 ppb for 1 min average, the NO at site B however can go down to 0.2 ppb.

[12] The NO_2 measured by the CAPS NO_2 monitor also tracks tightly with that measured by the CL-based analyzers ($r^2 = 0.91$, slope = 0.999, Figure 3b), yet noticeable differences in particular during afternoon were observed. Figure 3b shows that the differences between the CAPS and CL appear to be NO_z dependent. While the discrepancies are within ~10% when NO_z is below 8 ppb, large differences up to ~30% at high NO_z levels (> 14 ppb, Figure 3c) were observed between CAPS and CL because of the interferences of other reactive nitrogen species on CL NO_2 measurement. This is due to the well known sensitivity of the CL-based NO_2 measurements to organic nitrates and HNO_3, which depends upon inlet configuration and thermal operation range of a molybdenum or stainless steel converter [*Winer et al.*, 1974; *Parrish et al*., 1990; *Murphy et al*., 2007; *Kebabian et al*., 2008; *Steinbacher et al*., 2007]. At low NO_z levels (< 2 ppb), the CAPS NO_2 shows slightly higher values than that from CL. Although the band of 440 nm is essentially interference free, the 1,2-dicarbonyl compounds, e.g., glyoxal and methyl glyoxal can affect the accuracy of CAPS NO_2 measurements by absorbing in the same spectral region. Such interferences might be significant when the ratio of glyoxal to NO_2 is high. However, based on previous measurements of glyoxal and NO_2 at both urban and rural sites [*Volkamer et al*., 2005; *Li et al*., 2013], the interferences of glyoxal on the measurement of ambient NO_2 are generally less than 10%.

[13] Figure 4b shows the diurnal variation of NO_2 measured by the CAPS and CL for the entire study. While the NO_2 from two methods agree reasonably with each other at nighttime, large differences up to 20% were observed during daytime, mostly between 12:00 and 16:00. The large discrepancies in the afternoon are likely due to the overestimation of CL NO_2 because of the interferences of abundant reactive nitrogen species. In addition, the different sampling sites might also contribute to the observed differences in NO_2

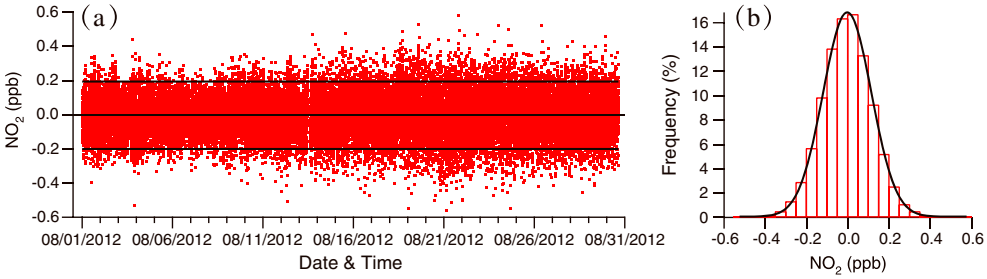

Figure 1. (a) Time series of NO_2 concentration (1 s data) measured from NO_2-free air every 1 h for the entire study, (b) Gaussian distribution of NO_2 in Figure 1a. The two solid lines in Figure 1a indicate the 10th and 90th percentiles of the data points.

measurements. We also note that the CAPS NO_2 sometimes shows higher concentration than the CL NO_2 at nighttime, which might be due to the interferences of some nitrogen containing species, e.g., peroxyacyl nitrates (PANs) and N_2O_5, which are not thermally stable and can decompose to NO_2 in the CAPS system [*Kebabian et al.*, 2008]. However, the discrepancies at nighttime (3.7%) are much smaller compared to those observed during daytime (17.4%).

3.2. Time Series and Diurnal Variations

[14] The time series of NO, NO_2, NO_y, NO_z, O_x, and particulate NO_3^-, as well as the solar radiation during the observation period is shown in Figure 2. The NO shows regular and prominent peaks in the early morning due to the traffic emissions in the morning rush hour. This is evident from the diurnal cycle of NO (Figure 4a), which shows a pronounced morning peak. The NO concentration peaks between 7:00 and 8:00 (~17 ppb) and then gradually decreases to a low ambient level (~ 1 ppb) due to the titration of NO by O_3, and also the rising boundary layer during the daytime [*Lin et al.*, 2008, 2011].

[15] The gaseous NO_2 also presents a pronounced diurnal cycle, yet the highest concentration occurs in the early morning and the lowest values appear between 14:00 and 15:00 (Figure 4b). The low concentration of NO_2 in the afternoon is due to the deep boundary layer [*Quan et al.*, 2013] and also the oxidation to NO_z, e.g., nitric acid, PAN, etc., consistent with the pronounced NO_z peak in the afternoon (Figure 5).

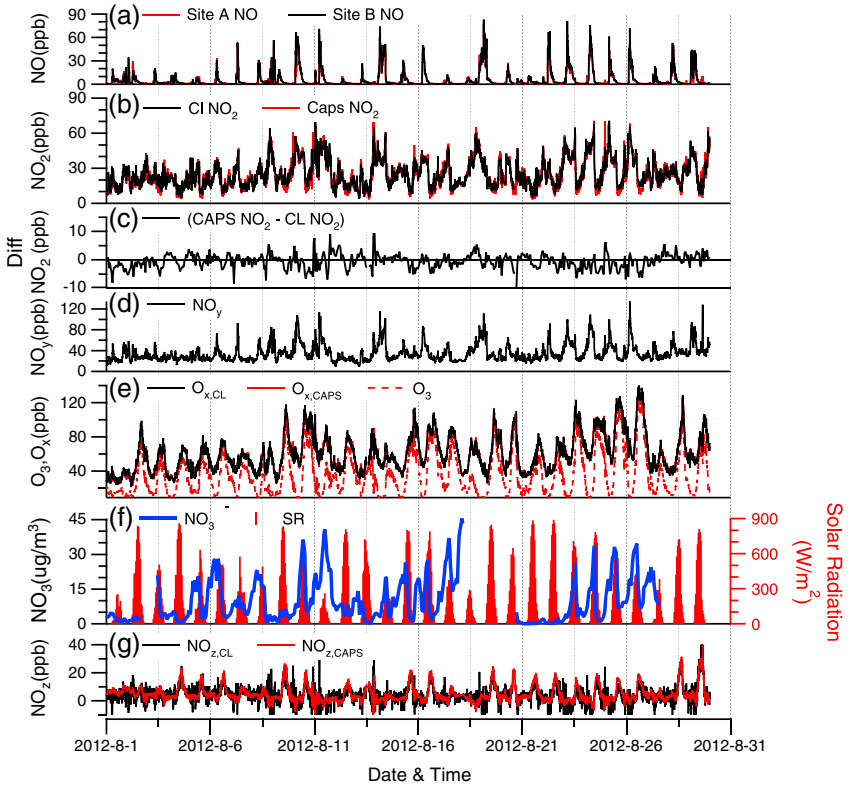

Figure 2. Time series of gaseous NO, NO_2, NO_y, O_3, O_x, and NO_z, particulate NO_3^- in submicron aerosols, and solar radiation (SR). The $NO_{z,CL}$ and $O_{x,CL}$ are $[NO_y] - [NO] - CL\ [NO_2]$ and $[O_3] + CL\ [NO_2]$, respectively, while The $NO_{z,CAPS}$ and $O_{x,CAPS}$ are $[NO_y] - [NO] - CAPS\ [NO_2]$ and $[O_3] + CAPS\ [NO_2]$, respectively.

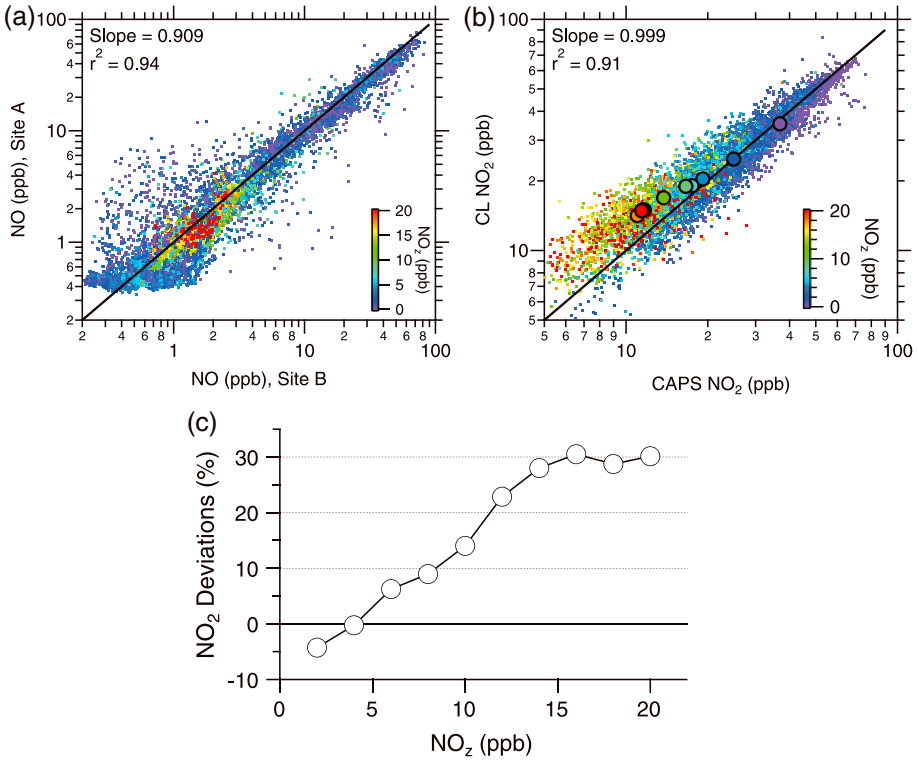

Figure 3. (a) Comparison of NO measured at site A and B; (b) Comparison of NO_2 measured by the CL NO_x analyzer at Site B and the CAPS NO_2 monitor at Site A; (c) NO_2 deviation between CAPS and CL versus NO_z. The data points are color coded with the NO_z concentration in Figures 3a and 3b. Also, the data points in Figure 3b are averaged according to NO_z concentration with 2 ppb increment (solid circles).

Figure 4c shows the diurnal cycles of NO_x and NO_y. Again, the diurnal profile of NO_x and NO_y shows a large gap during daytime with the max difference of ~15ppb at ~14:00, clearly indicating the photochemical production of NO_z. The photochemical formation of NO_z is strongly associated with solar radiation and O_3 mixing ratio. For example, the high O_3 pollution episodes, e.g., 9–10, 15–16, 19–26, and 28–29 August, show evident noon peaks, indicating the photochemical production of NO_z. However, the days with weak solar radiation (< 300 W m^{-2}) and low O_3, e.g., 1, 7–8, 12, 17–18, and 27 August, show correspondingly low production of NO_z. The relationship between O_x and NO_z will be further discussed in section 3.2

[16] Figure 5 shows the diurnal variations of $O_{x,CAPS}$ (= $[O_3]$ + CAPS $[NO_2]$) and $NO_{z,CAPS}$ (= $[NO_y]$ − $[NO]$ − CAPS $[NO_2]$), as well as the $O_{x,CL}$ (= $[O_3]$ + CL $[NO_2]$) and $NO_{z,CL}$ (= $[NO_y]$ − $[NO]$ − CL $[NO_2]$). The diurnal cycle of O_x is similar to NO_z with higher values appearing during the afternoon and lower ones at night and early morning. In addition to the photochemical production, regional transport might be another reason for the daytime peaks. For example, *Wang et al.* [2010b] found that regional pollution sources could contribute ~34–88% to the peak ozone at the urban site in Beijing. In this study, the average concentration of O_x for the second peak (15:00–18:00) was 79.4 and 54.4 ppb, respectively, from the air masses in the east-southwest and northeast. If assuming that the O_x from clean regions in the northeast represents a background level, the regional transport could contribute ~32% of O_x peak when the air masses are from the east-southwest, overall consistent with the results from *Wang et al.* [2010b].

3.3. Ozone Production Efficiency (OPE_x)

[17] The OPE_x is an important indicator to evaluate O_3-NO_x-VOCs sensitivity and to make effective O_3 control strategies in urban areas [*Couach et al.*, 2004; *Rickard et al.*, 2002; *Shiu et al.*, 2007; *Sillman*, 1999; *Xu et al.*, 2009; *Zaveri et al.*, 2003]. The OPE_x can be derived from the regression slopes of correlations between O_x and NO_z [*Kleinman et al.*, 1994; *Trainer et al.*, 1993]. Therefore, the accuracy of NO_2 measurement plays an important role in the calculation of OPE_x by influencing the quantification of O_x and NO_z. Using the same approach, the $OPE_{x,CAPS}$ and $OPE_{x,CL}$ were obtained from the correlation analysis of $[O_{x,CAPS}]$ versus $[NO_{z,CAPS}]$ and $[O_{x,CL}]$ versus $[NO_{z,CL}]$, respectively in this study. Hourly averaged data between 7:00 and 17:00 are used for the correlation analysis. In addition, only slopes with correlation coefficients $R > 0.6$ (significant level at 95%) and intercept > 0 (the background O_x concentration) are considered to be effective daily $OPE_{x,CAPS}$/$OPE_{x,CL}$ for this study. Given the general overestimation of CL NO_2 [*Steinbacher et al.*, 2007], the $OPE_{x,CL}$ calculated from the NO_y and NO_x measured by 42CTL analyzer would represent an upper limit of OPE_x, especially in the photochemically aged air [*Ge et al.*, 2010].

[18] Figure 6 shows the calculated daily $OPE_{x,CAPS}$ and $OPE_{x,CL}$ using 1 h average data for the entire study. It should be noted that some OPE_x values were missed in Figure 6 because the correlations of O_x versus NO_z in these days did

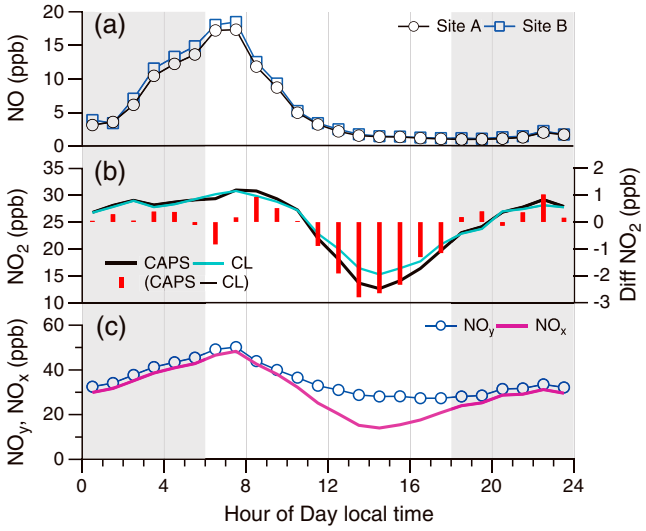

Figure 4. Mean diurnal cycles of (a) NO, (b) NO_2, and (c) NO_x and NO_y based on the entire measurement period.

not meet the requirements for calculation of OPE_x in this study. The daily $OPE_{x,CAPS}$ varies from 1.0 to 6.8 ppb/ppb with an average ($\pm 1\sigma$) of 2.6 (± 1.3) for the entire study. As a comparison, the $OPE_{x,CL}$ is generally higher than $OPE_{x,CAPS}$, ranging from 0.9 to 8.1. The average of $OPE_{x,CL}$ for the entire study is 3.4, which is ~30% higher than that of $OPE_{x,CAPS}$. The higher $OPE_{x,CL}$ is primarily due to the overestimation of the CL NO_2, leading to an over prediction of $[O_{x,CL}]$, and further a corresponding underestimation of $[NO_{z,CL}]$. As a result, the $OPE_{x,CL}$ calculated from the relationship between $[O_{x,CL}]$ and $[NO_{z,CL}]$ is overestimated. The discrepancies between $OPE_{x,CAPS}$ and $OPE_{x,CL}$ vary day by day, and the overestimation of $OPE_{x,CL}$ ranges from 19–37% depending on photochemical production of NO_z and the differences of NO_2 between CAPS and CL. Our results suggest that the previously reported OPE_x calculated from the CL measurements [*Xu et al.*, 2009; *Ge et al.*, 2012] might have been overestimated by 30% on average.

[19] Despite this, the $OPE_{x,CAPS}$ in this study overall falls within the OPE_x range previously reported in summer in Beijing (Table 1), for example, 3–6 [*Wang et al.*, 2006, 2010b] and 2.7–8.7 at the urban sites in Beijing[*Chou et al.*, 2009]. Also, the $OPE_{x,CAPS}$ in this study is close to those reported in other cities, e.g., 2.5–4 for Nashville urban plume [*Nunnermacker et al.*, 1998], 2.2–4.2 in New York City [*Kleinman et al.*, 2000], and slightly lower than the range of 3.9–4.7 observed in Los Angeles, California [*Pollack et al.*, 2012]. However, the OPE_x in Beijing during summertime is observed to be higher by a factor of 2.4 compared to wintertime [*Lin et al.*, 2011], indicating higher ozone production efficiency in summer than winter. It should be noted that the OPE_x in this study is generally lower than the values observed during Olympics 2008 [*Sun et al.*, 2011; *Chou et al.*, 2011]. One explanation for the higher OPE_x during the Olympic Games in 2008 is the different VOCs-NO_x-O_3 sensitivity. During the 2008 Olympics, the NO_x emission was reduced by 47% due to the strict controlling strategy [*Wang et al.*, 2010a]. The O_3 formation was likely shifted from VOC sensitive to NO_x sensitive [*Chou et al.*, 2011; *Sun et al.*, 2011]. Also, the low NO_x concentration generally would lead to the high OPE_x values (Figure 8). Another reason might be related to the well-known phenomenon commonly referred to as the "weekend ozone effect" or "holiday effect" [*Fujita et al.*, 2003; *Pollack et al.*, 2012; *Yarwood et al.*, 2003]. In these cases, *Chou et al.* [2011] and *Sun et al.* [2011] observed that enhancements in ozone are caused by reductions in NO_x emissions on weekends that lead to enhancements in VOC/NO_x ratio and ozone production efficiency. Although the high OPE_x values observed during the 2008 Olympics also coincided with weekends, the observed enhancements likely reflect changes in ozone precursors due to the short-term, but strict control policies implemented for this event. Note that the OPE_x varies differently among different O_3 episodes. Figure 7 shows the correlations of $[O_x]$ versus $[NO_z]$ during four O_3 episodes (hourly maximum $O_3 > 100$ ppb), i.e., 9–10, 15–16, 19–20, and 23–26 August. Although the daily OPE_x during every episode is similar, the average OPE_x for four episodes is quite different, for example, the highest OPE_x of 3.6 ppb/ppb is observed during the episode of 23–26 August, which is more than twice higher than 1.5 ppb/ppb during the episode of 15–16 August.

[20] The daily OPE_x in this study is always lower than the value suggested for O_3-VOC sensitivity ($OPE_x < 7$, [*Sillman*, 1995]), indicating that the ozone production in summer in Beijing is VOC-limited. Therefore, measures to control VOC emissions in Beijing would be effective to reduce O_3 levels. To further support this, we plot the daily OPE_x versus the peak of NO_x in early morning ($[NO_x]_0$, a surrogate of NO_x emissions from local traffic) in Figure 8. Similar to that reported by *Chou et al.* [2009] during the CAREBeijing-2006 campaign, the daily OPE_x presents a negative relationship with $[NO_x]_0$, suggesting that reduction of NO_x emissions appears not to be helpful for mitigation of O_3 pollution. The decrease of OPE_x as a function of $[NO_x]_0$ also supports the potential O_3-VOC sensitivity under the current ambient level of NO_x in Beijing. This is because that increase of $\Delta[NO_z]$ will not result in a corresponding increase of O_3 since high $[NO_x]_0$ is associated with high value of $\Delta[NO_z]$. $[NO_z]/[NO_y]$ is used to indicate the photochemical age by a number of studies [e.g., *Dommen et al.*, 1999; *Ge et al.*, 2012; *Kleinman et al.*, 2000; *Nunnermacker et al.*, 1998; *Olszyna et al.*, 1994]. The variations of daily OPE_x as a function of $[NO_z]/[NO_y]$ are shown in Figure 8b. The OPE_x shows a

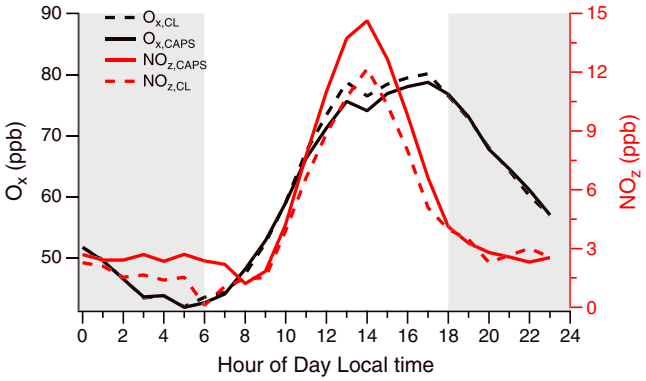

Figure 5. Mean diurnal cycles of $O_{x,CAPS}$, $O_{x,CL}$, $NO_{z,CAPS}$, and $NO_{z,CL}$ for the entire study. The shaded areas in the figure refer to nighttime.

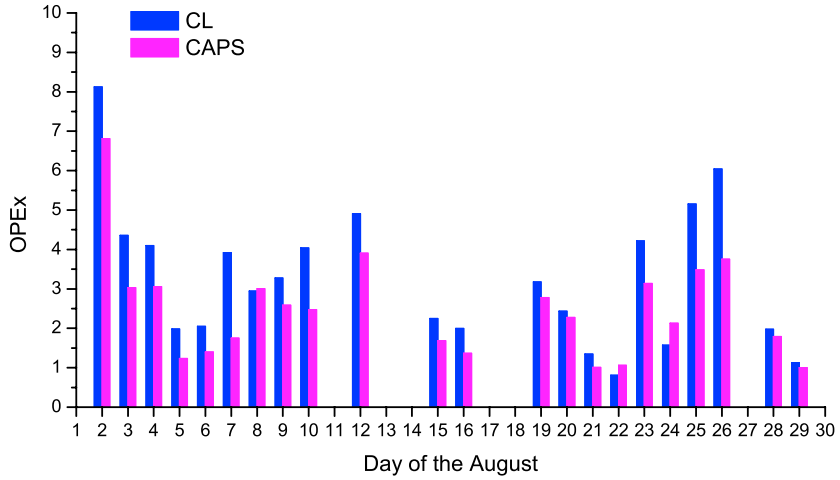

Figure 6. Time series of daily $OPE_{x,CAPS}$ and $OPE_{x,CL}$ derived from the correlations of $O_{x,CAPS}$ versus $NO_{z,CAPS}$, and $O_{x,CL}$ versus $NO_{z,CL}$, respectively.

positive correlation with $[NO_z]/[NO_y]$ ($r^2 = 0.38$, $p < 0.05$)), indicating that the OPE_x at the urban site of Beijing increases simultaneously with the aging of air parcels. This result is consistent with that observed at Peking University (near 4th North Ring of Beijing) during CAREBeijing-2006 [*Chou et al.*, 2009] and also in agreement with those at various urban sites, e.g., Houston and Tennessee, USA [*Daum et al.*, 2003; *Zaveri et al.*, 2003]. However, the correlation between OPE_x and $[NO_z]/[NO_y]$ is contrary to that observed at a rural site (SDZ) in Beijing, where ~75% of O_3 pollution is from regional transport rather than local photochemical production [*Ge et al.*, 2012].

3.4. Case Studies

[21] Our previous study frequently observed high concentration of nitrate in summer, which played an important role in particulate matter pollution in Beijing [*Sun et al.*, 2012]. Similarly, several episodes with high concentration of nitrate were also observed in this study (Figure 2). The formation of nitrate is mainly driven by three different processes, i.e., daytime photochemical production (R1), gas-particle partitioning (R2), and nighttime heterogeneous reactions (R3–R5). It appears that high concentration of NO_3^- is closely linked to the high O_3 and NO_2, which are two key precursors in the formation of nitrate particles. Here two high-O_3 episodes were chosen to further elucidate the roles of precursors of O_3 and NO_2 in the nitrate formation.

$$NO_2 + OH + M \rightarrow HNO_3(g) + M \quad \text{(R1)}$$

$$HNO_3(g) + NH_3(g) \Leftrightarrow NH_4NO_3(s) \quad \text{(R2)}$$

$$NO_2 + O_3 \rightarrow NO_3 + O_2 \quad \text{(R3)}$$

$$NO_2 + NO_3 + M \rightarrow N_2O_5 + M \quad \text{(R4)}$$

$$N_2O_5 + H_2O\ (aq) \rightarrow 2\ HNO_3 \quad \text{(R5)}$$

[22] The first high-O_3 episode (Ep1) occurred between 9–10 August (Figure 9). The daily maximum of O_3 showed a large enhancement from ~60 ppb on 8 August to ~100 ppb on 9–10 August, indicating the strong photochemical processing during the 2 days. Although the OPE_x values were similar, 2.6 and 2.5 ppb/ppb, respectively, the variations of nitrate in aerosol particles were quite different. The concentration of NO_3^- remained consistently low ($< 7\ \mu g\ m^{-3}$) on 9 August, yet exhibited a large enhancement associated with a pronounced diurnal cycle on 10 August. The increase of NO_3^- on 10 August showed a corresponding decrease of NO_y and NO. While the NO_3^- concentration was enhanced by a factor of more than 6 from ~6 $\mu g\ m^{-3}$ to 38 $\mu g\ m^{-3}$ in 6 h (6:00–12:00), the NO_y and NO decreased by ~53% and

Table 1. A Summary of the OPE_x Reported in Beijing and Surrounding Regions[a]

Location	OPE_x	Method	NO_2 Instrument	Date	References
Beijing, Mountain area	3–6	$[O_3]$ versus $[NO_y]$	P-CL	July 2005	*Wang et al.* [2006]
Beijing, Mountain area	3.0	$[O_x]$ versus $[NO_z]$	P-CL	Olympics, 2008	*Wang et al.* [2010b]
Beijing, Urban	1.1	$[O_x]$ versus $[NO_z]$	CL	Winter 2007	*Lin et al.* [2011]
Beijing, Urban	3.7–9.7	$[O_x]+[NO_z]$ versus $[NO_z]$	P-CL	Summer 2008	*Chou et al.* [2009]
Beijing, Urban	4–22	$[O_x]$ versus $[NO_z]$	P-CL	Olympics, 2008	*Sun et al.* [2011]
Beijing, Urban	8	$[O_x]+[NO_z]$ versus $[NO_z]$	P-CL	Olympics, 2008	*Chou et al.* [2011]
Beijing, Urban	1–6.8	$[O_x]$ versus $[NO_z]$	CAPS	Summer 2012	This study
Beijing, Rural area					
Urban plume	4.0	$[O_x]$ versus $[NO_z]$	CL	Summer 2008	*Ge et al.* [2012]
Rural plume	5.3	$[O_x]$ versus $[NO_z]$	CL	Summer 2008	*Ge et al.* [2012]
Nashville, Urban plume	2.5–4	$[O_x]$ versus $[NO_z]$	P-CL	July 1995	*Nunnermacker et al.* [1998]
New York, Urban	2.2–4.2	$[O_3]$ versus $[NO_z]$	P-CL	July 1996	*Kleinman et al.* [2000]
Los Angeles, California	3.9–4.7	$[O_x]$ versus $[NO_z]$	P-CL	May–June 2010	*Pollack et al.* [2012]

[a]P-CL represents the photolysis-chemiluninescence instruments.

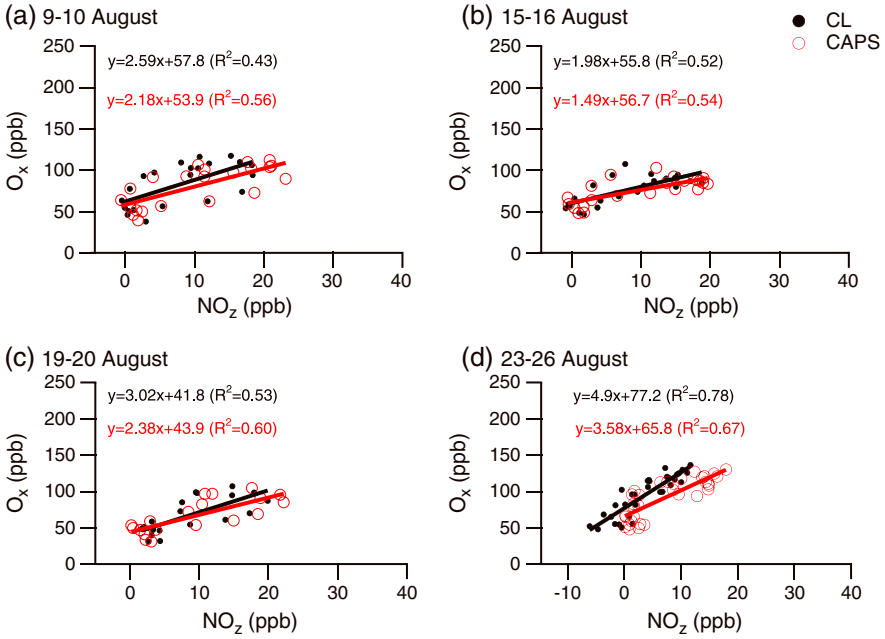

Figure 7. Correlations between $O_{x,CAPS}$ and $NO_{z,CAPS}$ (red dots), and $O_{x,CL}$ and $NO_{z,CL}$ (black dots) during four high-O_3 episodes: (a) 9–10 August, (b)14–15 August, (c)19–20 August, and (d) 23–26 August. The regression slopes refer to the average $OPE_{x,CAPS}$ (red dots) and $OPE_{x,CL}$ (black dots) determined for each episode.

85% to 47 and 9 ppb, respectively. It is very likely that the NO_3^- plume was due to the rapid photochemical production from the reactions of NO_2 and OH, followed by the formation of nitrate particles. In addition, the relatively low ambient temperature and high RH also facilitates the partitioning of HNO_3 to nitrate particles. After 12:00, the NO_3^- started to decrease rapidly mainly because of the evaporative loss of NH_4NO_3 at high ambient temperature, and also the deeper PBL. Although the variations of O_3 and meteorological variables were similar, the concentration of nitrate however was much lower on 9 August than on 10 August, which was likely due to the consistently low levels of NO_2 limiting the daytime photochemical production of nitrate from the reaction of NO_2 with OH.

[23] Beijing experienced another high-O_3 episode during 23–26 August (Ep2, Figure 10). During the 4 day episode, the variations of wind, RH and temperature were rather similar day by day, and the precursors of O_3 and NO_2 remained at high levels. The average OPE_x of 3.4 ppb/ppb is among the highest values throughout this study, suggesting the strong photochemical processing during this episode. Indeed, the daily maximum of O_3 is up to 130 ppb, which is the highest value observed in this study. To better elucidate the formation of nitrate, we calculate the photochemical production rate of HNO_3 using $NO_2 \times UV$ as a surrogate during daytime and the equilibrium constant of K_p for the reaction R2 (higher K_p indicates more stable NH_4NO_3) [*Seinfeld and Pandis*, 2006]. The time series of $NO_2 \times UV$ and K_p is shown in Figure 11.

[24] The NO_3^- presented two peaks occurring in the early morning and around noon, and it appeared that the evolution of NO_3^- was separated into two stages, i.e., from midnight to ~3:00–4:00, and from ~5:00–6:00 to noon. During the first stage, the increase of NO_3^- was associated with a synchronous increase of NO_2 and a corresponding decrease of O_3.

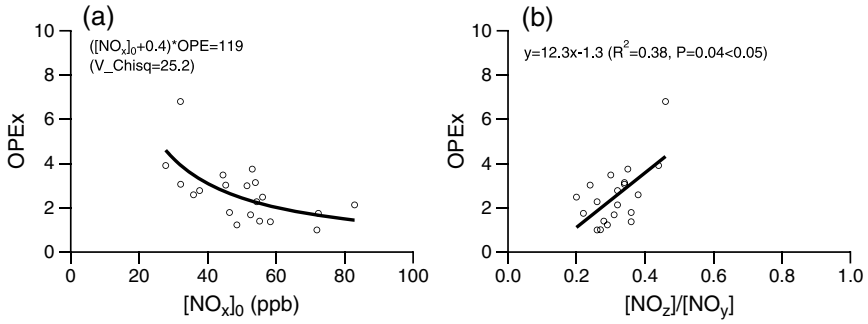

Figure 8. Correlations of (a) OPE_x versus $[NO_x]_0$, and (b) OPE_x versus $[NO_z]/[NO_y]$. $[NO_x]_0$ is the maximum of NO_x in early morning representing the relative traffic emission of 1 day. $[NO_z]/[NO_y]$ indicates the photochemical age of the air, and higher values suggest more aged air.

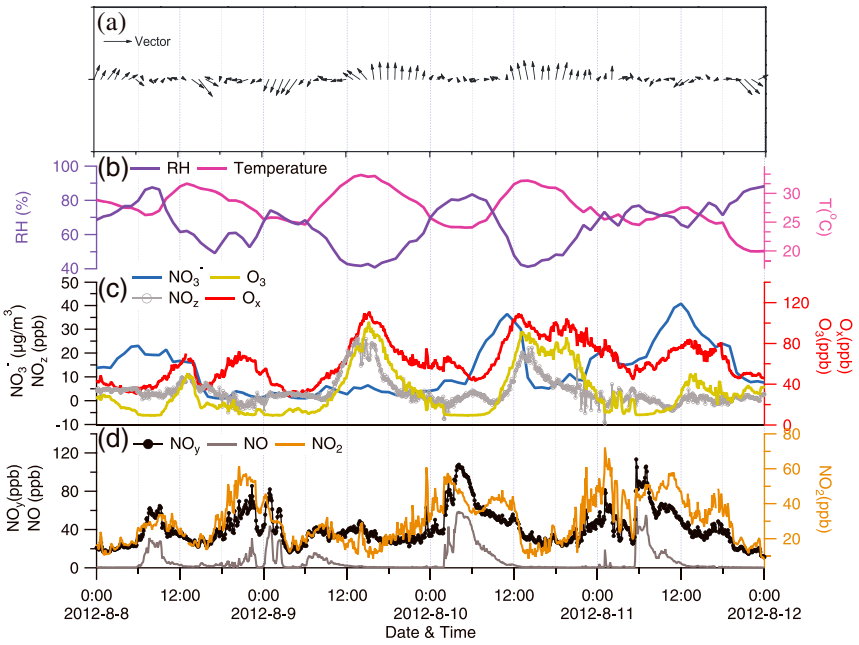

Figure 9. Time series of (a) wind vector, (b) RH and temperature , (c) particulate NO_3^-, NO_z, O_3, and O_x, (d) NO, NO_2, and NO_y during 8–11 August.

While the NO was low, the NO_2 and O_3 remained at a considerable level, which facilitated the formation of the NO_3 radical and dinitrogen pentoxide (R3–R4), and hence the heterogeneous formation of HNO_3 under high RH conditions. This is consistent with the continuous increase of the equilibrium constant of K_p for ammonium nitrate formation. Although the low boundary layer height might have played a role in the enhancement of NO_3^- concentration, the first peak at ~3:00–4:00 was more likely due to the heterogeneous reaction associated with the removal of NO_x at nighttime. The formation of NO_3 was then slowed down because the precursor of O_3 was almost completely consumed during this period. The NO_3^- started to increase again at ~5:00–6:00 and peaked between ~10:00–12:00. The increase of NO_3^-

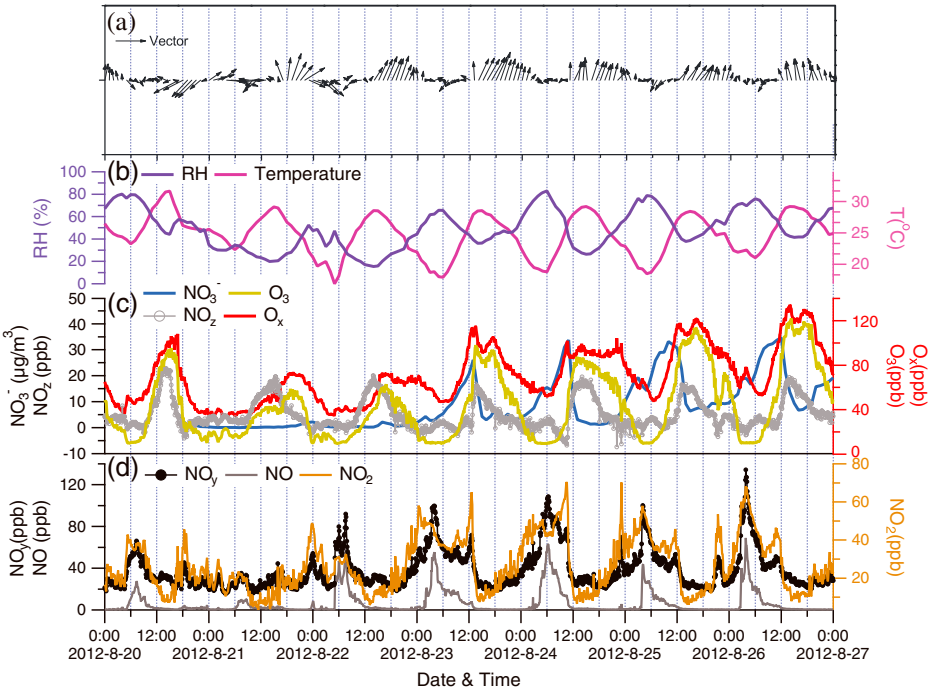

Figure 10. Same as Figure 9, but during 20–26 August.

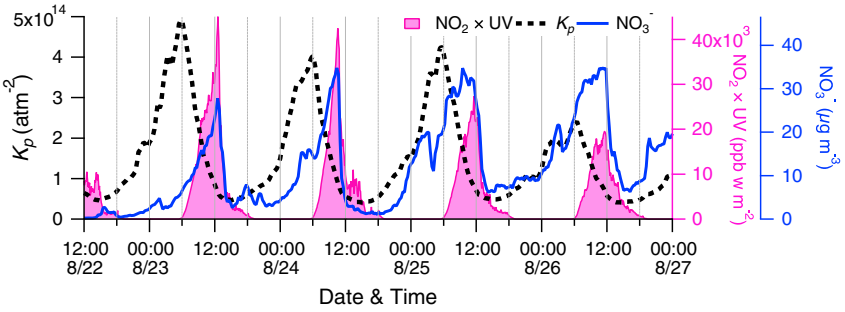

Figure 11. Time series of particulate NO_3^-, equilibrium constant of K_p for ammonium nitrate formation, and $NO_2 \times UV$, a surrogate of photochemical production rate of HNO_3 during daytime.

exactly corresponded to the start of daytime photochemical processing ($NO_2 \times UV$ in Figure 11). Meanwhile, the K_p gradually decreased counteracting the formation of nitrate. Therefore, the second increase of NO_3^- suggests the photochemical production dominates over the evaporative loss processes during this stage. The photochemical production reached a maximum at noon time when the NO_3^- concentration peaked as well. After that, the NO_3^- rapidly decreased to the lowest level of the day in ~2–3 h, due to the reduced photochemical production rate and significantly enhanced evaporative loss.

4. Conclusions

[25] The ambient nitrogen dioxide (NO_2) was measured in situ by an Aerodyne Cavity Attenuated Phase Shift NO_2 monitor in August 2012 at an urban site in Beijing. The CAPS is highly sensitive with the detection limit an order of magnitude lower than the standard, commercially available CL-based NO_x analyzer, and also a wide linear response range of 15 ppt–1 ppm. The NO_2 measured by the CAPS and CL shows overall agreement; however, large discrepancies up to ~20%, in particular during the afternoon, were also observed due to the interferences with reactive nitrogen species on CL measurements. The discrepancies therefore were NO_z dependent with larger differences associated at higher NO_z levels.

[26] The daily OPE_x was derived from the correlation of O_x versus NO_z. The average OPE_x for the entire study was 2.6 (1–6.8) ppb/ppb, which is comparable to the values previously reported in Beijing. Our results showed that the OPE_x derived from the CL NO_2 can be overestimated by 19–37% due to the interferences with reactive nitrogen species. The overestimation is expected to be more significant in rural and remote areas where the contribution of NO_z to the total NO_y is much higher than urban cities. The generally low OPE_x and the negative correlation between OPE_x and $[NO_x]_0$ implied the VOC-limited ozone production in summer in Beijing. In addition, the OPE_x increased as a function of photochemical age, $[NO_z]/[NO_y]$, which is in contrast to that observed at rural sites, indicating the different sources and photochemical processing of O_3 between urban and rural areas in and around Beijing.

[27] Two case studies during 9–10 August and 23–26 August 2012 revealed that high concentrations of precursors of O_3 and NO_2 are of importance for the formation of nitrate particles. A detailed analysis of the evolution of gaseous species, nitrate, and meteorological conditions suggest that the variations of nitrate in fine particles are caused by the competing effects of different formation mechanisms, including daytime photochemical production, gas-particle partitioning equilibrium, and nighttime heterogeneous reactions. Overall, high concentrations of NO_2 and O_3 with favorable meteorological conditions, e.g., high RH and low temperature, will greatly facilitate the formation of nitrate particles and increase the air pollution levels in the cities.

[28] **Acknowledgments.** This work was supported by the National Natural Science Foundation of China (41175108 & 41225019), the National Key Project of Basic Research (2013CB955801), and the Strategic Priority Research Program (B) of the Chinese Academy of Sciences (grant XDB05020501 & grant XDB05030203). This work was also partly supported by Academia Sinica through grants AS-102-SS-A10. We thank the Technical and Service Center, Institute of Atmospheric Physics, Chinese Academy of Sciences for providing the meteorology data.

References

Chameides, W. L., et al. (1992), Ozone precursor relationships in the ambient atmosphere, *J. Geophys. Res.*, *97*, 6037–6055.

Chou, C. C. K., C. Y. Tsai, C. J. Shiu, S. C. Liu, and T. Zhu (2009), Measurement of NO_y during Campaign of Air Quality Research in Beijing 2006 (CAREBeijing-2006): Implications for the ozone production efficiency of NO_x, *J. Geophys. Res.*, *114*, D00G01, doi:10.1029/2008JD010446.

Chou, C. C. K., C. Y. Tsai, C. C. Chang, P. H. Lin, S. C. Liu, and T. Zhu (2011), Photochemical production of ozone in Beijing during the 2008 Olympic Games, *Atmos. Chem. Phys.*, *11*(18), 9825–9837.

Couach, O., F. Kirchner, R. Jimenez, I. Balin, S. Perego, and H. van den Bergh (2004), A development of ozone abatement strategies for the Grenoble area using modeling and indicators, *Atmos. Environ.*, *38*(10), 1425–1436, doi:10.1016/j.atmosenv.2003.12.001.

Daum, P. H., L. I. Kleinman, S. R. Springston, L. J. Nunnermacker, Y. N. Lee, J. Weinstein-Lloyd, J. Zheng, and C. M. Berkowitz (2003), A comparative study of O_3 formation in the Houston urban and industrial plumes during the 2000 Texas Air Quality Study, *J. Geophys. Res.*, *108*(D23), 4715, doi:10.1029/2003jd003552.

Dommen, J., A. S. H. Prévôt, A. M. Hering, T. Staffelbach, and G. L. Kok (1999), Photochemical production and aging of an urban air mass, *J. Geophys. Res.*, *104*, 5493–5506.

Dunlea, E. J., et al. (2007), Evaluation of nitrogen dioxide chemiluminescence monitors in a polluted urban environment, *Atmos. Chem. Phys.*, *7*(10), 2691–2704.

Fujita, E. M., W. R. Stockwell, D. E. Campbell, R. E. Keislar, and D. R. Lawson (2003), Evolution of the magnitude and spatial extent of the weekend ozone effect in California's South Coast Air Basin, 1981–2000, *J. Air Waste Manage.*, *53*(7), 802–815.

Ge, B., X. Xu, W. Lin, and Y. Wang (2010), Observational study of ozone production efficiency at the Shangdianzi Regional Background Station (in Chinese with English abstract), *Environ. Sci.*, *31*(7), 1444–1450.

Ge, B. Z., X. B. Xu, W. L. Lin, J. Lie, and Z. F. Wang (2012), Impact of the regional transport of urban Beijing pollutants on downwind areas in summer: Ozone production efficiency analysis, *Tellus B*, *64*, 17,348–17,351, doi:10.3402/tellusb.v64i0.17348.

Guttikunda, S. K., G. R. Carmichael, G. Calori, C. Eck, and J. H. Woo (2003), The contribution of megacities to regional sulfur pollution in Asia, *Atmos. Environ.*, *37*(1), 11–22.

Guttikunda, S. K., Y. H. Tang, G. R. Carmichael, G. Kurata, L. Pan, D. G. Streets, J. H. Woo, N. Thongboonchoo, and A. Fried (2005), Impacts of Asian megacity emissions on regional air quality during spring 2001, *J. Geophys. Res.*, *110*, D20301, doi:10.1029/2004JD004921.

Hao, J. M., L. T. Wang, L. Li, J. N. Hu, and X. C. Yu (2005), Air pollutants contribution and control strategies of energy-use related sources in Beijing, *Sci. China Ser. D*, *48*, 138–146.

Kanakidou, M., et al. (2011), Megacities as hot spots of air pollution in the East Mediterranean, *Atmos. Environ.*, *45*(6), 1223–1235.

Kebabian, P. L., S. C. Herndon, and A. Freedman (2005), Detection of nitrogen dioxide by cavity attenuated phase shift spectroscopy, *Anal. Chem.*, *77*(2), 724–728.

Kebabian, P. L., E. C. Wood, S. C. Herndon, and A. Freedman (2008), A practical alternative to chemiluminescence-based detection of nitrogen dioxide: Cavity attenuated phase shift spectroscopy, *Environ. Sci. Technol.*, *42*(16), 6040–6045.

Kleinman, L., et al. (1994), Ozone formation at a rural site in the southeastern United States, *J. Geophys. Res.*, *99*, 3469–3482.

Kleinman, L. I., P. H. Daum, D. G. Imre, J. H. Lee, Y.-N. Lee, L. J. Nunnermacker, S. R. Springston, J. Weinstein-Lloyd, and L. Newman (2000), Ozone production in the New York City urban plume, *J. Geophys. Res.*, *105*, 14,495–14,511.

Lawrence, M. G., T. M. Butler, J. Steinkamp, B. R. Gurjar, and J. Lelieveld (2007), Regional pollution potentials of megacities and other major population centers, *Atmos. Chem. Phys.*, *7*(14), 3969–3987.

Li, X., T. Brauers, A. Hofzumahaus, K. Lu, Y. P. Li, M. Shao, T. Wagner, and A. Wahner (2013), MAX-DOAS measurements of NO_2, HCHO and CHOCHO at a rural site in Southern China, *Atmos. Chem. Phys.*, *13*(4), 2133–2151.

Lin, W., X. Xu, X. Zhang, and J. Tang (2008), Contributions of pollutants from North China Plain to surface ozone at the Shangdianzi GAW Station, *Atmos. Chem. Phys.*, *8*, 5889–5898.

Lin, W., X. Xu, B. Ge, and X. Liu (2011), Gaseous pollutants in Beijing urban area during the heating period 2007–2008: Variability, sources, meteorological, and chemical impacts, *Atmos. Chem. Phys.*, *11*(15), 8157–8170, doi:10.5194/acp-11-8157-2011.

Liu, S. C., M. Trainer, F. C. Fehsenfeld, D. D. Parrish, E. J. Williams, D. W. Fahey, G. Hubler, and P. C. Murphy (1987), Ozone production in the rural troposphere and the implications for regional and global ozone distributions, *J. Geophys. Res.*, *92*(D4), 4191–4207.

Madronich, S. (2006), Chemical evolution of gaseous air pollutants downwind of tropical megacities: Mexico City case study, *Atmos. Environ.*, *40*(31), 6012–6018.

Molina, M. J., and L. T. Molina (2004), Megacities and atmospheric pollution, *J. Air Waste Manage.*, *54*(6), 644–680.

Molina, L. T., et al. (2010), An overview of the MILAGRO 2006 Campaign: Mexico City emissions and their transport and transformation, *Atmos. Chem. Phys.*, *10*(18), 8697–8760.

Murphy, J. G., D. A. Day, P. A. Cleary, P. J. Wooldridge, D. B. Millet, A. H. Goldstein, and R. C. Cohen (2007), The weekend effect within and downwind of Sacramento. Part 1: Observations of ozone, nitrogen oxides, and VOC reactivity, *Atmos. Chem. Phys.*, *7*(20), 5327–5339.

Nunnermacker, L. J., et al. (1998), Characterization of the Nashville urban plume on July 3 and July 18, 1995, *J. Geophys. Res.*, *103*, 28,129–28,148.

Olszyna, K. J., E. M. Bailey, R. Simonaitis, and J. F. Meagher (1994), O_3 and NO_y relationships at a rural site, *J. Geophys. Res.*, *99*(D7), 14,557–14,563.

Parrish, D. D., et al. (1990), Systematic variations in the concentration of NO_x (NO Plus NO_2) at Niwot-Ridge, Colorado, *J. Geophys. Res.*, *95*(D2), 1817–1836.

Pollack, I. B., B. M. Lerner, and T. B. Ryerson (2010), Evaluation of ultraviolet light-emitting diodes for detection of atmospheric NO_2 by photolysis-chemiluminescence, *J. Atmos. Chem.*, *65*, 111–125.

Pollack, I. B., et al. (2012), Airborne and ground-based observations of a weekend effect in ozone, precursors, and oxidation products in the California South Coast Air Basin, *J. Geophys. Res.*, *117*, D00V05, doi:10.1029/2011JD016772.

Quan, J. N., Y. Gao, Q. Zhang, X. X. Tie, J. J. Cao, S. Q. Han, J. W. Meng, P. F. Chen, and D. L. Zhao (2013), Evolution of planetary boundary layer under different weather conditions, and its impact on aerosol concentrations, *Particuology*, *11*(1), 34–40.

Ran, L., et al. (2012), Ozone production in summer in the megacities of Tianjin and Shanghai, China: A comparative study, *Atmos. Chem. Phys.*, *12*(16), 7531–7542.

Rickard, A. R., G. Salisbury, P. S. Monks, A. C. Lewis, S. Baugitte, B. J. Bandy, K. C. Clemitshaw, and S. A. Penkett (2002), Comparison of measured ozone production efficiencies in the marine boundary layer at two European coastal sites under different pollution regimes, *J. Atmos. Chem.*, *43*, 107–134.

Roberts, J. M., et al. (1995), Relationships between Pan and ozone at sites in eastern North America, *J. Geophys. Res.*, *100*(D11), 22,821–22,830.

Ryerson, T. B., E. J. Williams, and F. C. Fehsenfeld (2000), An efficient photolysis system for fast-response NO_2 measurements, *J. Geophys. Res.*, *105*(D21), 26,447–26,461.

Sadanaga, Y., Y. Fukumori, T. Kobashi, M. Nagata, N. Takenaka, and H. Bandow (2010), Development of a selective light-emitting diode photolytic NO_2 converter for continuously measuring NO_2 in the atmosphere, *Anal. Chem.*, *82*(22), 9234–9239.

Seinfeld, J. H., and S. N. Pandis (2006), *Atmospheric Chemistry and Physics: From Air Pollution to Climate Change*, 1203 pp., Wiley, New York.

Shao, M., X. Tang, Y. Zhang, and W. Li (2006), City clusters in China: Air and surface water pollution, *Front. Ecol. Environ.*, *4*(7), 353–361.

Shiu, C. J., S. C. Liu, C. C. Chang, J. P. Chen, C. C. K. Chou, C. Y. Lin, and C. Y. Young (2007), Photochemical production of ozone and control strategy for Southern Taiwan, *Atmos. Environ.*, *41*(40), 9324–9340, doi:10.1016/j.atmosenv.2007.09.014.

Sillman, S. (1995), The use of NO_y, H_2O_2 and HNO_3 as indicators for ozone-NO_x -hydrocarbon sensitivity in urban locations, *J. Geophys. Res.*, *100*, 14,175–14,188.

Sillman, S. (1999), The relation between ozone, NO_x and hydrocarbons in urban and polluted rural environments, *Atmos. Environ.*, *33*(12), 1,821–1,845.

Steinbacher, M., C. Zellweger, B. Schwarzenbach, S. Bugmann, B. Buchmann, C. Ordonez, A. S. H. Prevot, and C. Hueglin (2007), Nitrogen oxide measurements at rural sites in Switzerland: Bias of conventional measurement techniques, *J. Geophys. Res.*, *112*, D11307, doi:10.1029/2006JD007971.

Sun, Y., L. L. Wang, Y. S. Wang, L. Quan, and Z. R. Liu (2011), In situ measurements of SO_2, NO_x, NO_y, and O_3 in Beijing, China during August 2008, *Sci. Total Environ.*, *409*(5), 933–940.

Sun, Y. L., Z. F. Wang, H. B. Dong, T. Yang, J. Li, X. L. Pan, P. Chen, and J. T. Jayne (2012), Characterization of summer organic and inorganic aerosols in Beijing, China with an Aerosol Chemical Speciation Monitor, *Atmos. Environ.*, *51*, 250–259.

Sun, Y. L., Z. F. Wang, P. Q. Fu, T. Yang, Q. Jiang, H. B. Dong, J. Li, and J. J. Jia (2013), Aerosol composition, sources and processes during wintertime in Beijing, China, *Atmos. Chem. Phys.*, *13*, 4577–4592, doi:10.5194/acp-13-4577-2013.

Trainer, M., et al. (1993), Correlation of ozone with NO_y in photochemically aged air, *J. Geophys. Res.*, *98*(D2), 2917–2925.

Volkamer, R., L. T. Molina, M. J. Molina, T. Shirley, and W. H. Brune (2005), DOAS measurement of glyoxal as an indicator for fast VOC chemistry in urban air, *Geophys. Res. Lett.*, *32*, L08806, doi:10.1029/2005GL022616.

Wang, T., A. Ding, J. Gao, and W. S. Wu (2006), Strong ozone production in urban plumes from Beijing, China, *Geophys. Res. Lett.*, *33*, L21806, doi:10.1029/2006GL027689.

Wang, S. X., M. Zhao, J. Xing, Y. Wu, Y. Zhou, Y. Lei, K. B. He, L. X. Fu, and J. M. Hao (2010a), Quantifying the air pollutants emission reduction during the 2008 Olympic Games in Beijing, *Environ. Sci. Technol.*, *44*(7), 2490–2496.

Wang, T., et al. (2010b), Air quality during the 2008 Beijing Olympics: Secondary pollutants and regional impact, *Atmos. Chem. Phys.*, *10*(16), 7,603–7,615, doi:10.5194/acp-10-7603-2010.

Winer, A. M., J. W. Peters, J. P. Smith, and J. N. Pitts Jr (1974), Response of commercial chemiluminescent nitric oxide-nitrogen dioxide analyzers to other nitrogen-containing compounds, *Environ. Sci. Technol.*, *8*, 1118–1121.

Xu, X. B., B. Z. Ge, and W. L. Lin (2009), Progresses in research of Ozone Production Efficiency (OPE), *Adv. Earth Sci.*, *24*(8), 845–853.

Yarwood, G., T. E. Stoeckenius, J. G. Heiken, and A. M. Dunker (2003), Modeling weekday/weekend Los Angeles region for 1997, *J. Air Waste Manage.*, *53*(7), 864–875.

Zaveri, R. A., C. M. Berkowitz, L. I. Kleinman, S. R. Springston, P. V. Doskey, W. A. Lonneman, and C. W. Spicer (2003), Ozone production efficiency and NO_x depletion in an urban plume: Interpretation of field observations and implications for evaluating O_3-NO_x-VOC sensitivity, *J. Geophys. Res.*, *108*(D14), 4436, doi:10.1029/2002jd003144.